Support Information

Degradation of Carbamazepine by HF-Free-Synthesized MIL-101(Cr)@Anatase TiO₂ Composite under UV-A irradiation: Degradation mechanism, wastewater matrix effect and degradation pathway

J. W. Goh[1], Y. Xiong[1], W. Wu[2], Z. Huang[2], S. L. Ong[1] and J. Y. Hu[1]*

[1]Department of Civil & Environmental Engineering, National University of Singapore, 1 Engineering Drive 2, Singapore 117576

[2]Singapore Institute of Manufacturing Technology, 2 Fusionopolis Way #08-04 Innovis Singapore 138634

*Corresponding author: Email: hujiangyong@nus.edu.sg

Text. S1. Chemicals & reagents

Table. S1. Types of APIs identified in pharmaceutical effluents and their corresponding concentrations

Table. S2. Surrogate parameters of pharmaceutical wastewater samples

Table. S3. Total alkalinity as $CaCO_3$ (mg/L) of pharmaceutical wastewater samples

Table. S4. Cl^- and SO_4^{2-} in pharmaceutical wastewater samples

Table. S5. GC/MS temperature program (DB 1301)

Table. S6. GC/MS temperature program (Mega-Wax)

Table. S7. Weight % & Atomic % of each element based on TEM EDS Point Detection Location

Table. S8. Common chemical states of Cr and corresponding binding energy

Table. S9. Isotherm & kinetic model parameters for adsorption of CBZ onto MIL-101(Cr)

Table. S10. Adsorption kinetic parameters for TiO_2: MIL-101(Cr) composites with varied ratio

Table. S11. Pseudo-steady state •OH concentration $[OH]ss$ due to TiO_2:MIL composites with varied ratio

Table. S12. Rate constants for hydroxyl radical trapping ($k_{rxn/•OH}$)

Table. S13. Redox potentials for oxidizing species

Table. S14. Rate of reaction of •OH radicals with selected amides in aqueous solution

Table. S15. Possible intermediates of CBZ with their elemental composition & structure

Table. S16. Intermediates identified due to various quenchers in excess at 50-minute reaction

Figure S1. GC/MS spectrum of pharmaceutical wastewater samples PWS 1 & PWS 2 using (A) DB1301, (C) Mega-Wax with MS spectrum of (B) Tetrahydrofuran & (D) N, N Dimethyl-Formamide

Figure S2. (A) Calibration curve & (B) Absorbance spectrum of CBZ by HPLC-DAD at 285nm wavelength

Text. S1. Chemicals & reagents

Carbamazepine ($C_{15}H_{12}N_2O$, > 99%), tert-butanol ($C_4H_{10}O$, ≥ 99.5%), potassium iodide (KI, ≥ 99%), sodium azide (NaN_3, ≥ 99.5%), *p*-benzoquinone ($C_6H_4O_2$, ≥ 98%), silver nitrate ($AgNO_3$, ≥ 99%), DMPO ($C_6H_{11}NO$, ≥ 97%), ethanol (C_2H_6O, ≥ 99.8%), chromium (III) nitrate nonahydrate ($Cr(NO_3)_3 \cdot 9H_2O$, 99%), terephthalic acid (H_2BDC, 98%), N,N-dimethylformamide (C_3H_7NO, 99.8%), titanium (IV) butoxide (TBOT, 97%), sodium hydroxide (NaOH, ≥ 98%), sulfuric acid (H_2SO_4, > 99%), sodium chloride (≥ 99.5%), sodium sulfate (> 99%), sodium bicarbonate ($NaHCO_3$, > 99%), sodium carbonate (Na_2CO_3, ≥ 99.5%) were purchased from Sigma-Aldrich. All solutions used were made with ultrapure water with a resistivity of > 18MΩ from a Synergy 185 water purification system (Millipore, USA).

Table. S1. Types of APIs identified in pharmaceutical effluents and their corresponding concentrations

Country	Pharmaceuticals Identified	Concentration	References
Korea	Carbamazepine Acetylsalicylic Acid Diclofenac Lincomycin Sulfamethazine	0.001mg/L 0.551mg/L 0.181mg/L 0.114mg/L 0.166mg/L	[1]
Israel	Carbamazepine Venlafaxine	0.84±0.19mg/L 11.72±2.2mg/L	[2]
India	Carbamazepine Oxcarbazepine	2.21 ± 0.1 mg/L 5.54 ± 0.19 mg/L	[3]

Table. S2. Surrogate parameters of pharmaceutical wastewater samples

Parameters	PWS 1		PWS 2	
	Min – Max	Average	Min – Max	Average
pH	10.50 – 10.80	10.70	11.30 – 11.70	11.58
COD (mg/L)	70,000 – 93,000	86,742	130,000 – 210,000	170,341
TOC (mg/L)	16,100 – 25,700	20,149	68,700 – 90,100	78,011
Total Dissolved Solids (mg/L)	6,000 – 6,600	6,287.88	85,000 – 125,000	109,024.13

Table. S3. Total alkalinity as $CaCO_3$ (mg/L) of pharmaceutical wastewater samples

Parameters	PWS 1		PWS 2	
	Min – Max	Average	Min – Max	Average
Total Alkalinity as $CaCO_3$ (mg/L)	1,000 – 1,130	1,098.56	43,200 – 44,600	43,839.11

Table. S4. Cl^- and SO_4^{2-} in pharmaceutical wastewater samples

Ion species	PWS 1		PWS 2	
	Range	Average	Range	Average
Cl^-, mg/L	2,900 – 3,400	3,160.46	26,000 – 45,600	31,163.37
SO_4^{2-}, mg/L	-	-	1,200 – 2,000	1,551.38

Table. S5. GC/MS temperature program (DB 1301)

GC-MS system (Model: GCMS-QP2010, Shimadzu, Japan)		
GC-Column: DB1301 column (Low to mid polarity; Length (30cm) x Diameter (0.24mm I.D) x Film (0.25μm))		
a. Temperature	GC Injector	250ºC
	Oven Initial	35ºC (4 min holding)
	Oven Ramping Rate	4ºC per min for a total of
	Oven Maximum	200ºC for 10 min holding
b. Flow rate	Column (He)	1.2 mL/min
	Split	12 mL/min
c. MS System	Ionization mode	EI (70eV)
	Ion Source Temp.	200ºC
	Interface Temp.	200ºC
	TIC Scan Range	35 – 250 m/z
	Threshold	100

Table. S6. GC/MS temperature program (Mega-Wax)

GC-MS system (Model: GCMS-QP2010, Shimadzu, Japan)		
GC-Column: Megawax (High Polarity; Length (30cm) x Diameter (0.25 mm I.D) x Film (0.25µm))		
a. Temperature	GC Injector	230°C
	Oven Initial	40°C (2 min holding)
	Oven Ramping Rate	15°C per min for a total of 13.33 min
	Oven Maximum	200°C for 10 min holding
b. Flow rate	Column (He)	1.2 mL/min
	Split	12 mL/min
c. MS System	Ionization mode	EI (70eV)
	Ion Source Temp.	230°C
	Interface Temp.	230°C
	TIC Scan Range	30 – 300 m/z
	Threshold	0

Table. S7. Weight % & Atomic % of each element based on TEM EDS Point Detection Location

MIL-101(Cr)@TiO$_2$ Composite	Titanium (Ti)		Oxygen (O)		Chromium (Cr)	
	Weight %	Atomic %	Weight %	Atomic %	Weight %	Atomic %
Location 2	0.38	0.16	72.41	89.49	27.19	10.34
Location 4	27.85	12.69	60.34	82.34	11.80	4.95
Location 5	15.86	6.94	65.18	85.41	18.95	7.64

Table. S8. Common chemical states of Cr and corresponding binding energy

Chemical State	Binding Energy Cr2p$_{3/2}$ / eV
Cr Metal	574.3
Cr (III) oxide	576
Cr (VI) oxide	579

Table. S9. Isotherm & kinetic model parameters for adsorption of CBZ onto MIL-101(Cr)

Langmuir Adsorption Isotherm			Freundlich Adsorption Isotherm		
Q$_m$ (mg/g)	K$_L$ (L/mg)	R^2	K$_F$ (mg/g)(L/g)^n	n	R^2
18.195	0.0306	0.9969	0.640	1.2138	0.9975
Pseudo 1st Order Kinetic (Lagergren)			Pseudo 2nd Order Kinetic (Ho & Mckay)		
q$_e$ (mg/g)	k$_1$ (min^{-1})	R^2	q$_e$ (mg/g)	k$_2$ (g/mg.min)	R^2
3.908	0.3209	0.9452	4.424	0.0934	0.9898

Table. S10. Adsorption kinetic parameters for varied percentage of TiO$_2$: MIL-101(Cr) composite

X% TiO$_2$: MIL-101(Cr)	Pseudo 1st Order Kinetic (Lagergren)			Pseudo 2nd Order Kinetic (Ho & Mckay)		
	q$_e$ (mg/g)	k$_1$ (min^{-1})	R^2	q$_e$ (mg/g)	k$_2$ (g/mg.min)	R^2
MIL-101(Cr)	3.908	0.3210	0.9521	4.424	0.0934	0.9798
2.29%	2.515	0.2675	0.9929	2.917	0.1069	0.9930
4.58%	2.566	0.4237	0.9397	2.945	0.1282	0.9598
9.17%	1.754	0.4237	0.9619	1.965	0.2874	0.9551
13.75%	1.869	0.1542	0.9827	2.354	0.0617	0.9843
18.33%	1.910	0.1626	0.9452	2.490	0.0383	0.9661

Table. S11. Pseudo-steady state •OH concentration [OH]ss by TiO_2:MIL composites with varied ratio

X% TiO_2: MIL-101(Cr)	[•OH]$_{ss}$	R^2
2.29%	1.12428E-13	0.8880
4.58%	2.7733E-13	0.9980
9.17%	4.27788E-13	0.9696
13.75%	4.01515E-13	0.9865
18.33%	3.80781E-13	0.9926

Table. S12. Rate constants for hydroxyl radical trapping ($k_{rxn/•OH}$)

Spin Trap	$K_{rxn/•OH}$ (10^9)	References
Terephthalic Acid	4.4 ± 0.1	[4]
DMPO	3.4	[5]
Ethanol/Methanol	1.2 – 2.8	[6], [7]
Tert-Butanol	0.38-0.76	[8]
pCBA	5.0	[9]

Table. S13. Redox potentials for oxidizing species

Redox Pair	E^o (V) vs. NHE	Reference
$SO_4^{•-}/SO_4^{2-}$	2.43	[10]
$Cl_2^{•-}/2Cl^-$	2.10	[11]
$CO_3^{•-},H^+/HCO_3^-$	1.78	[12]

Table. S14. Rate of reaction of •OH radicals with selected amides in aqueous solution

Amides	$k_{•OH}$ (M^{-1} s^{-1})
Formamide	5.0×10^8
N-Methyl-Formamide (NMF)	1.2×10^9
N, N Dimethyl-Formamide (DMF)	1.7×10^9
Dimethyl-Acetamide (DMAc)	3.5×10^9
Acetamide	1.9×10^8

Table. S15. Possible intermediates of CBZ with their elemental composition & structure

m/z [M+H]+	Name of Products	Elemental Composition	Structure	m/z [M+H]+	Name of Products	Elemental Composition	Structure
237	CBZ	$C_{15}H_{12}N_2O$		253	P252	$C_{15}H_{12}N_2O_2$	
180	Acridine	$C_{13}H_9N$		196	Acridone /P195	$C_{13}H_9NO$	
225	P224	$C_{14}H_{12}N_2O$		223	P222	$C_{14}H_{10}N_2O$	
271	Trans-CBZ	$C_{15}H_{14}N_2O_3$		267	TP266/BQD	$C_{15}H_{10}N_2O_3$	
120	P119	$C_6H_5N_3$		251	BQM/P250	$C_{15}H_{10}N_2O_2$	
208	P207	$C_{14}H10NO$					

Table. S16. Intermediates identified due to various quenchers in excess at 50-minute reaction

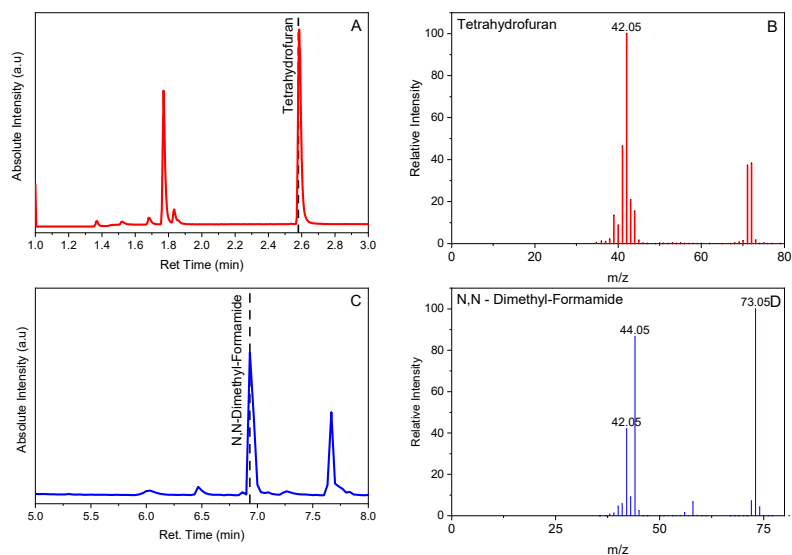| Conditions	Quenchers	Intermediates Formed
I	Blank	m/z = 237, 253, 251, 271, 180, 196, 120, 223, 225,267
II	KI (h$^+$)	m/z = 237
III	BQ (O$_2^{\bullet-}$)	m/z = 237, 253, 208
IV	Tert-Butanol (•OH)	m/z = 237, 253, 251, 271, 180, 196, 223, 267

Figure S1. GC/MS spectrum of pharmaceutical wastewater samples PWS 1 & PWS 2 using (A) DB1301, (C) Mega-Wax with MS spectrum of (B) Tetrahydrofuran & (D) N, N Dimethyl-Formamide
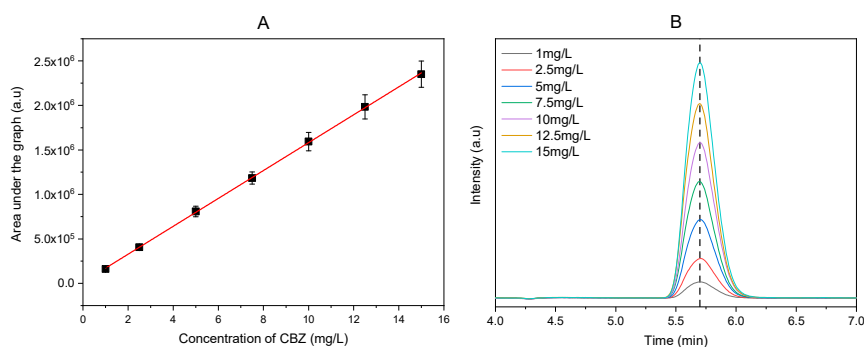
Figure S2. (A) Calibration curve & (B) Absorbance spectrum of CBZ by HPLC-DAD at 285nm wavelength
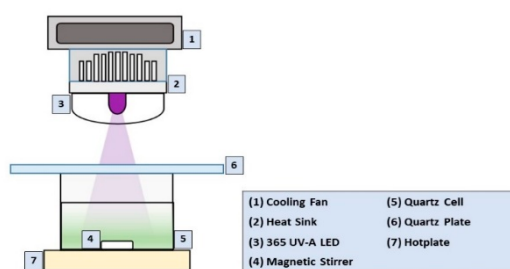
Figure S3. Schematic diagram of UV-A/LED photocatalytic setup
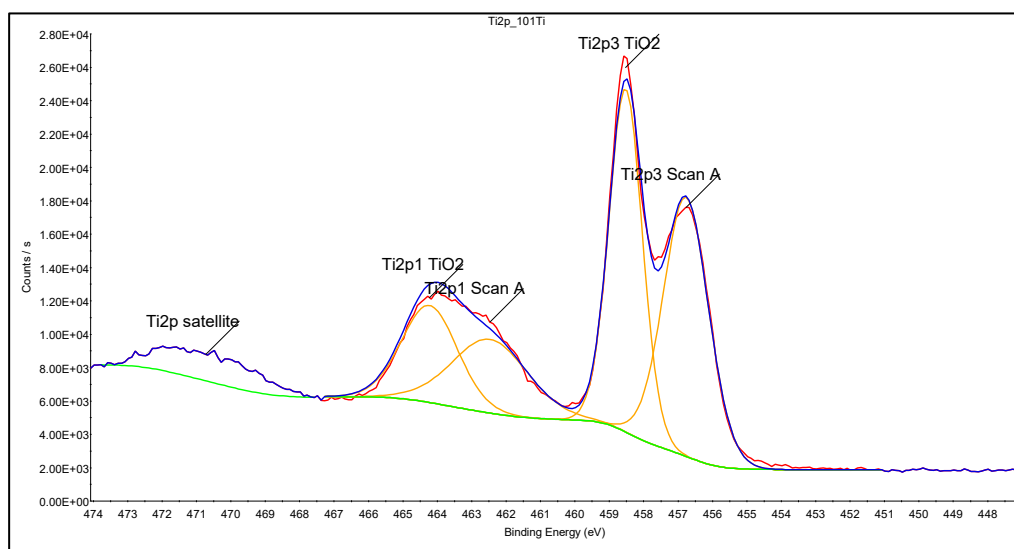
Figure S4. XPS patterns of MIL-101(Cr)@TiO$_2$ (Ti2p)
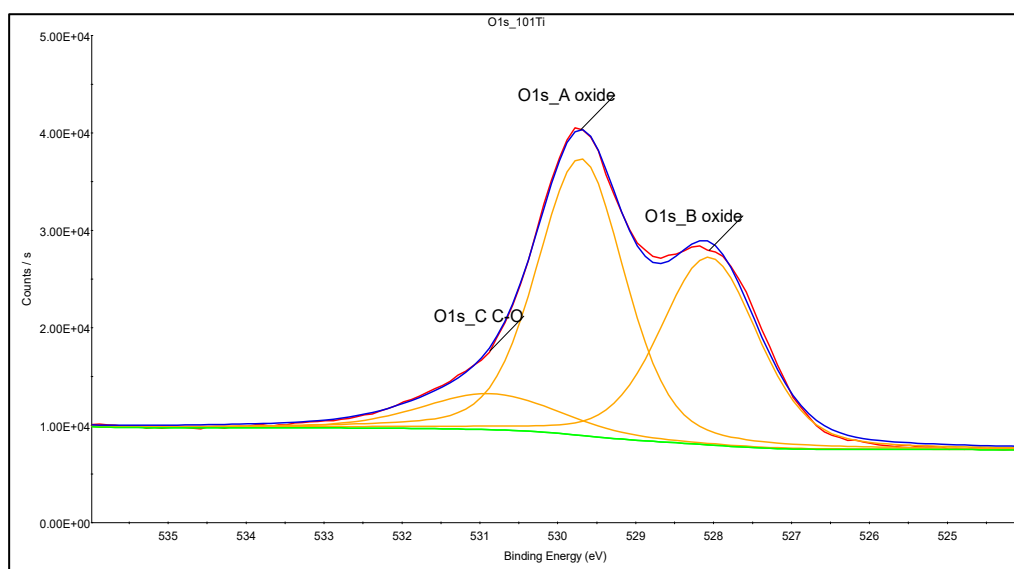
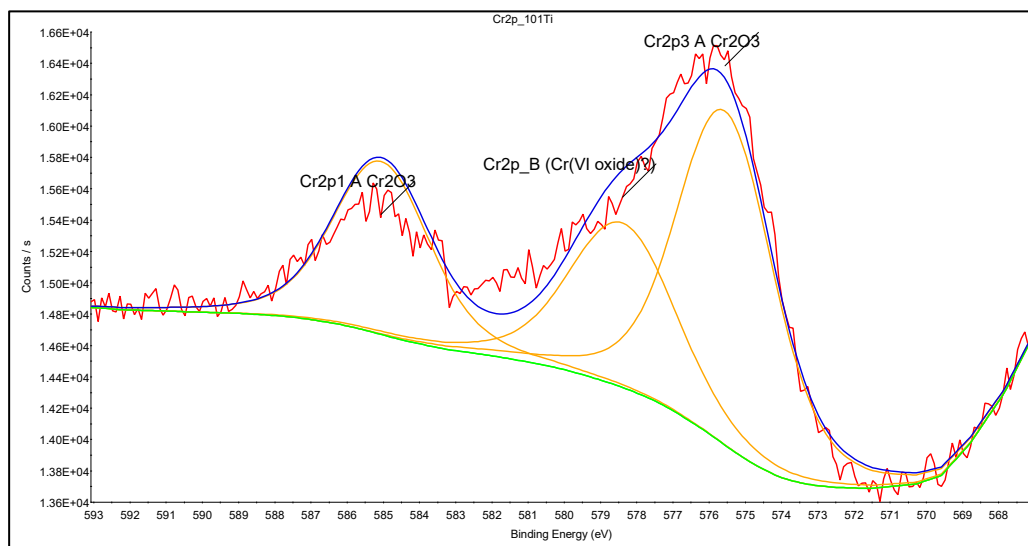**Figure S5.** XPS patterns of MIL-101(Cr)@TiO$_2$ (O1s)

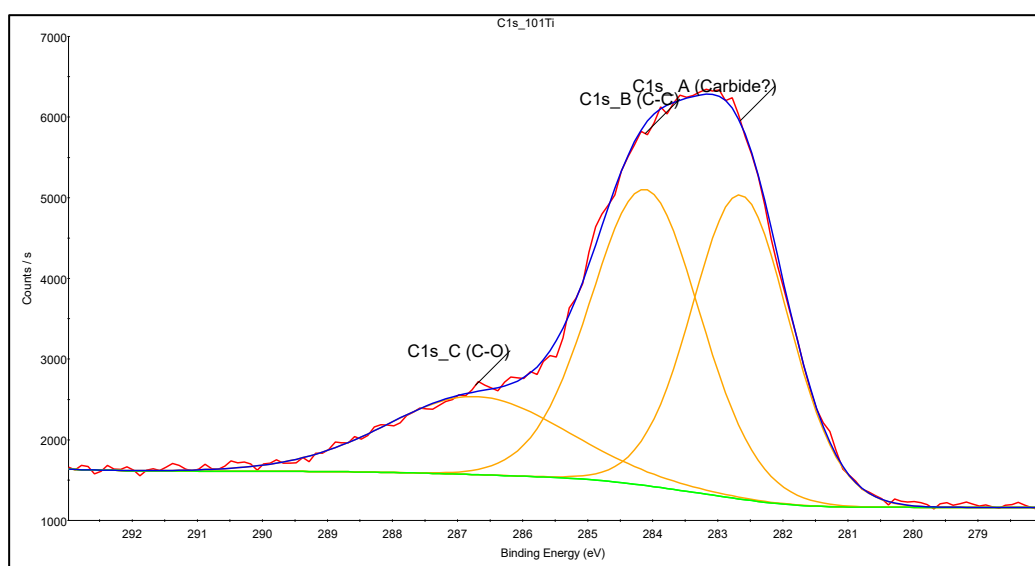**Figure S6.** XPS patterns of MIL-101(Cr)@TiO$_2$ (Cr2p)

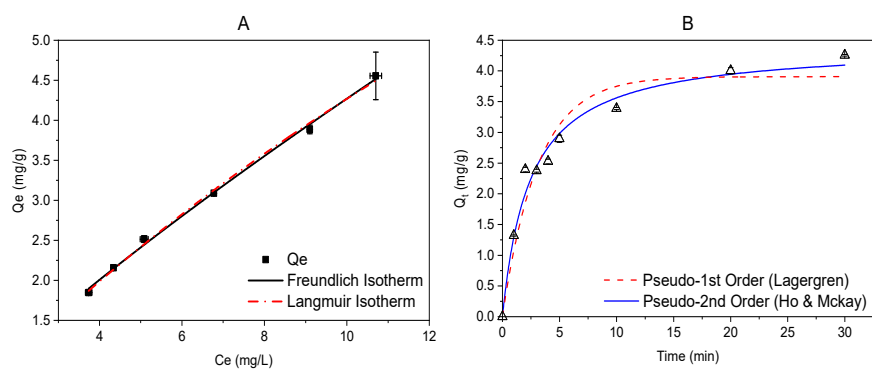**Figure S7.** XPS patterns of MIL-101(Cr)@TiO$_2$ (C1s)

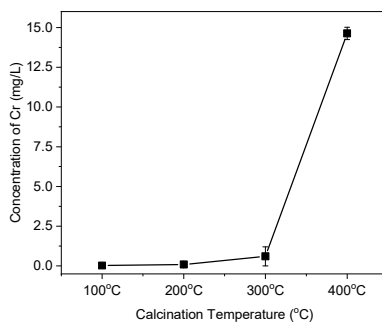**Figure S8.** (A) Adsorption isotherms (B) Adsorption kinetics of CBZ on MIL-101(Cr)

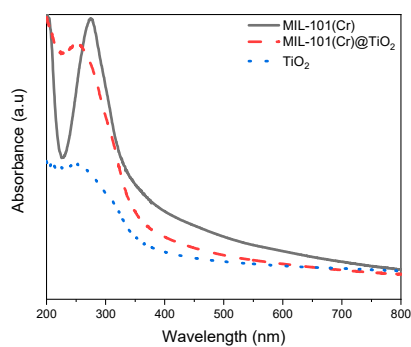**Figure S9.** Determination of Cr concentration using ICP-OES

Figure S10. Absorbance spectra of MIL-101(Cr), MIL-101(Cr)@TiO$_2$ and TiO$_2$
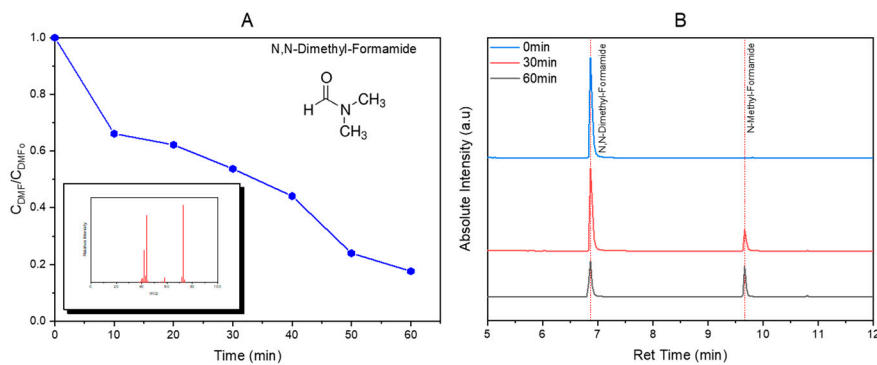

Figure S11. (A) Degradation of DMF using MIL-101(Cr)@TiO$_2$ with the corresponding MS Spectrum (B) GC/MS spectrum at different time intervals with presence of both DMF & N-Methyl-Formamide
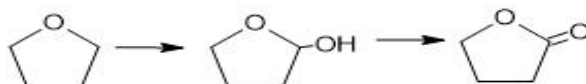

Figure S12. Transformation of tetrahydrofuran to 2-hydroxytetrahydrofuran to butyrolactone
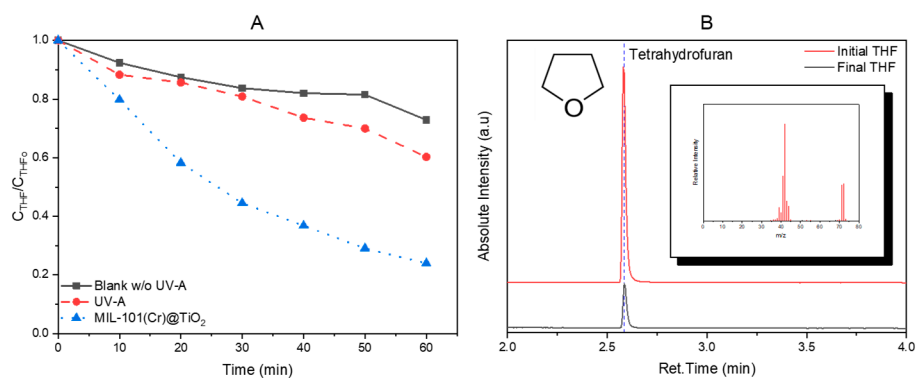
Figure S13. (A) Degradation of THF using MIL-101(Cr)@TiO$_2$ (B) GC/MS spectrum with the corresponding MS spectrum
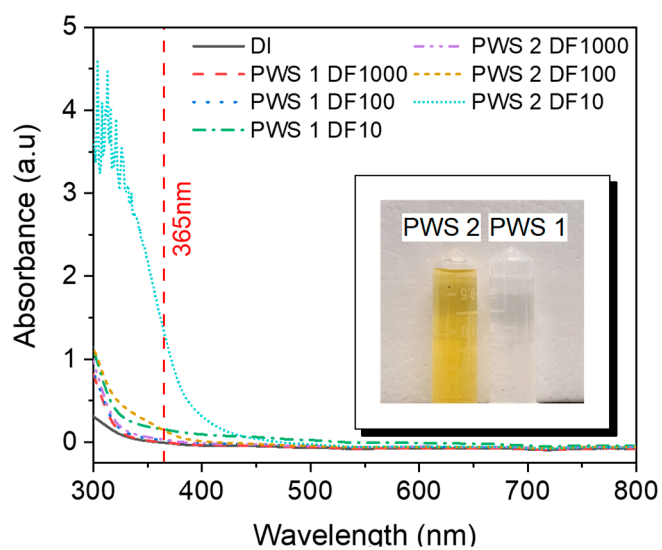

Figure S14. Absorbance spectrum of pharmaceutical wastewater samples PWS 1 & PWS 2 with different dilution factors
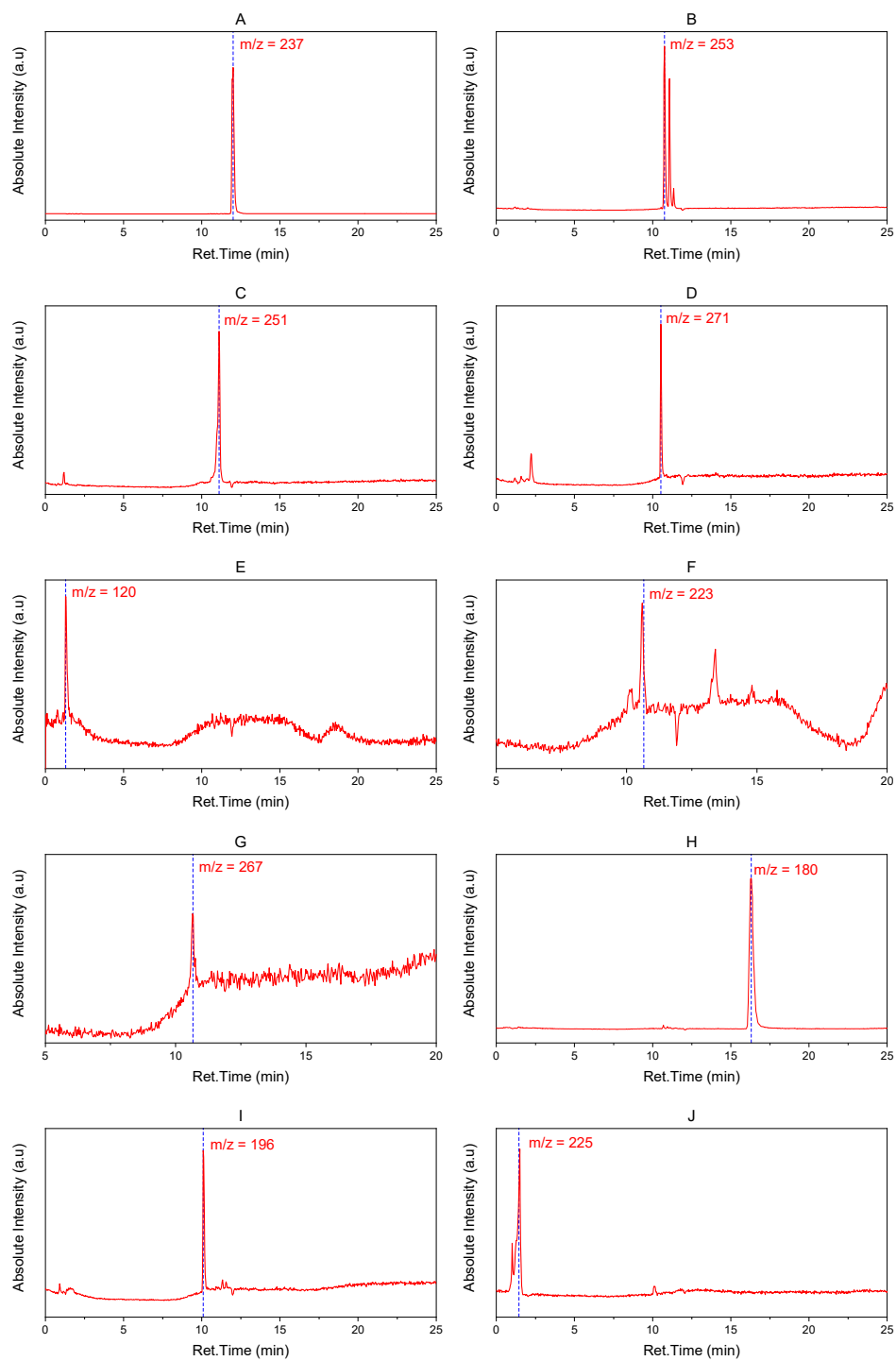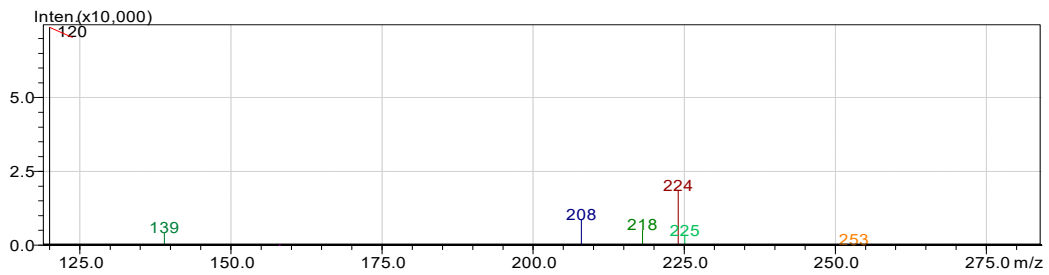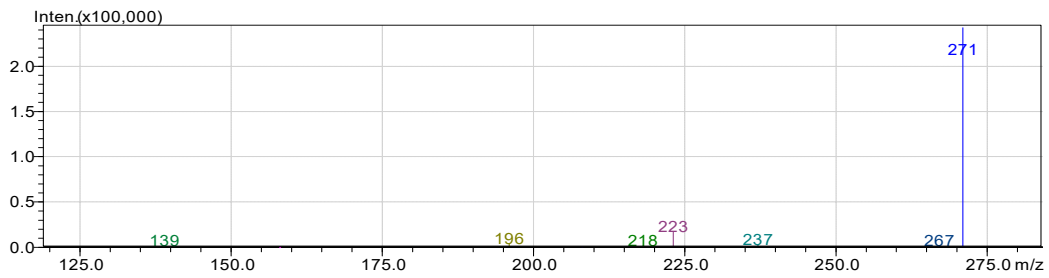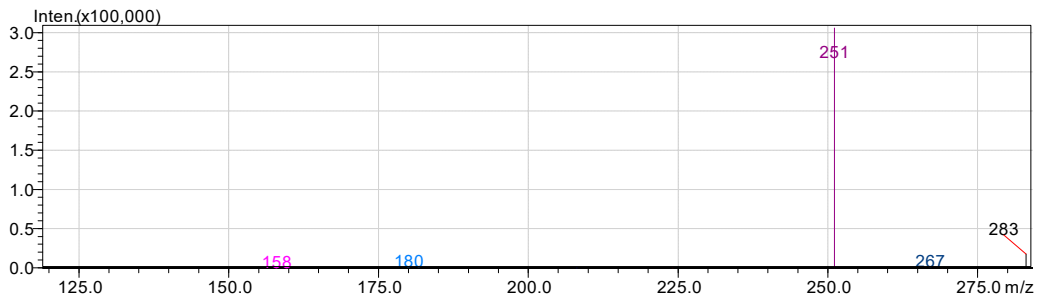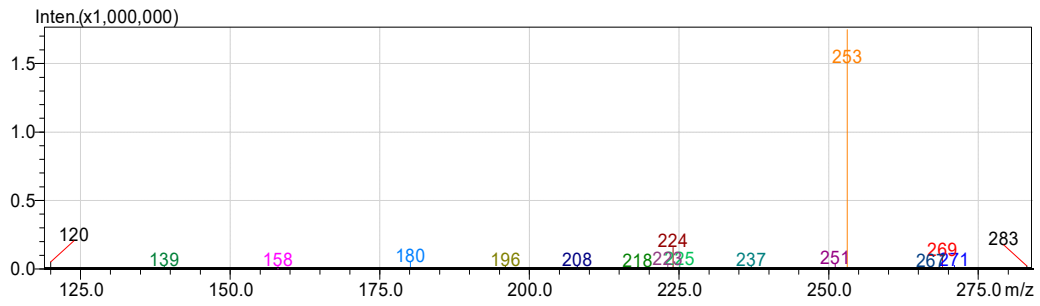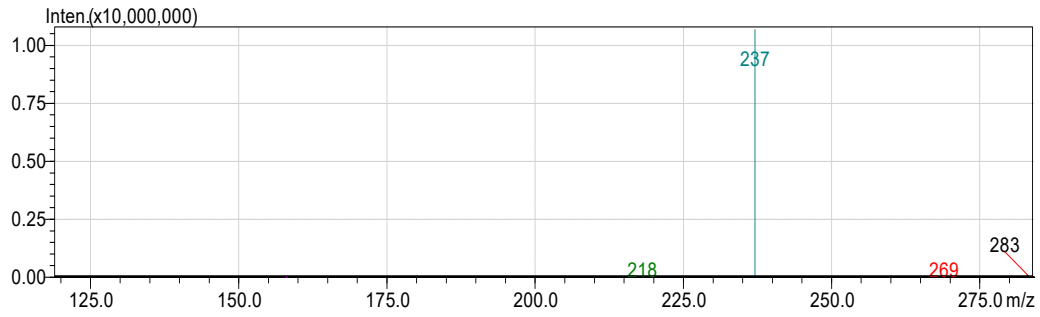
Figure S15. MS chromatography of CBZ & its intermediates: (A) m/z = 237 (B) m/z = 253 (C) m/z = 251 (D) m/z = 271 (E) m/z = 120 (F) m/z = 223 (G) m/z = 267 (H) m/z = 180 (I) m/z = 196 (J) m/z = 225

Inten.(x10,000,000)

1.00

0.75

0.50

0.25

0.00

237

218   269   283

125.0   150.0   175.0   200.0   225.0   250.0   275.0 m/z

Inten.(x1,000,000)

1.5   253

1.0

0.5

120   139   158   180   196   208 218 225 237   251   269 271 283

0.0

224

267

125.0   150.0   175.0   200.0   225.0   250.0   275.0 m/z

Inten.(x100,000)

3.0

2.5   251

2.0

1.5

1.0

0.5   283

0.0   158   180   267

125.0   150.0   175.0   200.0   225.0   250.0   275.0 m/z

Inten.(x100,000)

271

2.0

1.5

1.0

0.5   139   196   218 223 237   267

0.0

125.0   150.0   175.0   200.0   225.0   250.0   275.0 m/z

Inten.(x10,000)

120

5.0

2.5   224

208 218 225

139   253

0.0

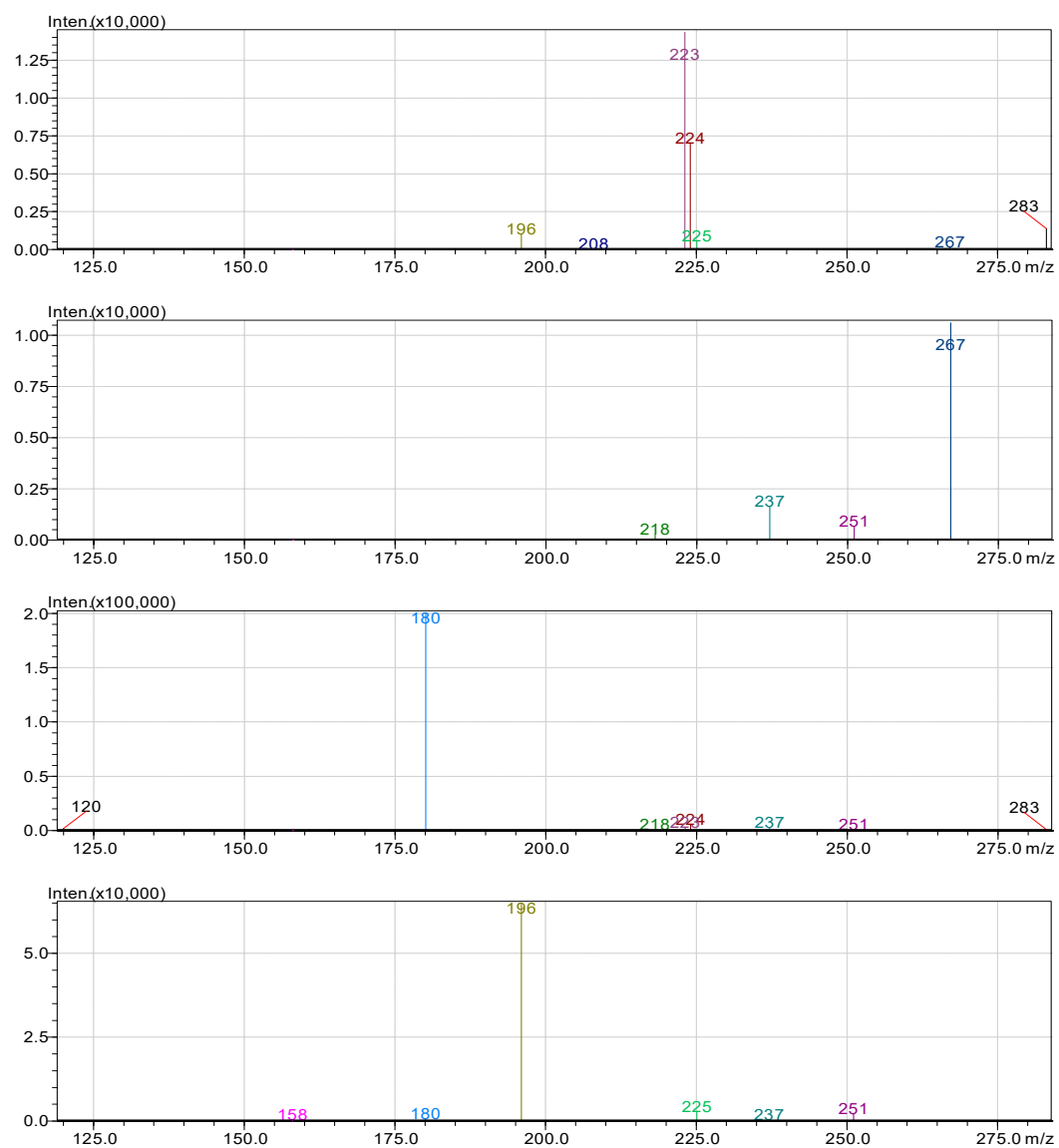125.0   150.0   175.0   200.0   225.0   250.0   275.0 m/z

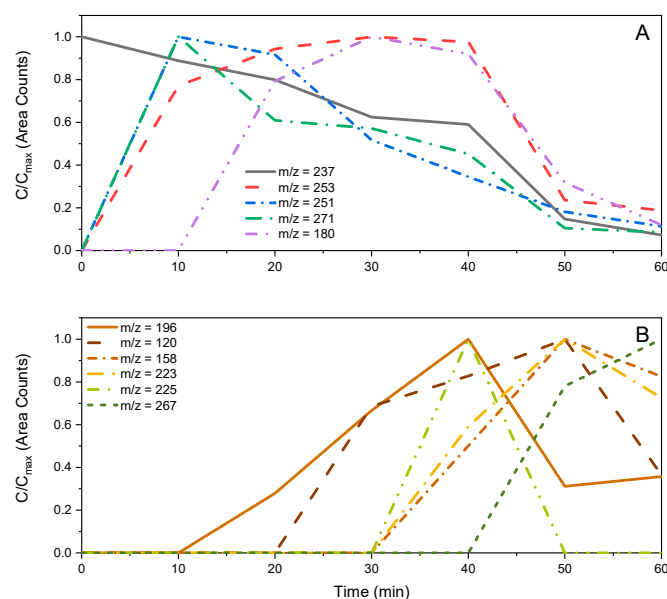**Figure S16.** MS spectrum of CBZ and its intermediates

Figure S17. Time-profiles of CBZ intermediates for MIL-101(Cr)@TiO$_2$ composite with UV-A irradiation (Max-Normalized)

References:

[1] W.-J. Sim, J.-W. Lee, E.-S. Lee, S.-K. Shin, S.-R. Hwang, and J.-E. Oh, "Occurrence and distribution of pharmaceuticals in wastewater from households, livestock farms, hospitals and pharmaceutical manufactures," *Chemosphere*, vol. 82, no. 2, pp. 179–186, 2011.

[2] Y. Lester, H. Mamane, I. Zucker, and D. Avisar, "Treating wastewater from a pharmaceutical formulation facility by biological process and ozone," *Water Res.*, vol. 47, no. 13, pp. 4349–4356, 2013.

[3] K. Dwivedi, A. Morone, V. Pratape, T. Chakrabarti, and R. A. Pandey, "Carbamazepine and oxcarbazepine removal in pharmaceutical wastewater treatment plant using a mass balance approach: A case study," *Korean J. Chem. Eng.*, vol. 34, no. 10, pp. 2662–2671, 2017.

[4] S. E. Page, W. A. Arnold, and K. McNeill, "Terephthalate as a probe for photochemically generated hydroxyl radical," *J. Environ. Monit.*, vol. 12, no. 9, pp. 1658–1665, 2010.

[5] E. Finkelstein, G. M. Rosen, and E. J. Rauckman, "Spin trapping of superoxide and hydroxyl radical: practical aspects," *Arch. Biochem. Biophys.*, vol. 200, no. 1, pp. 1–16, 1980.

[6] X. Hu, H. Dong, Y. Zhang, B. Fang, and W. Jiang, "Mechanism of N, N-dimethylformamide electrochemical oxidation using a Ti/RuO 2–IrO 2 electrode," *RSC Adv.*, vol. 11, no. 13, pp. 7205–7213, 2021.

[7] Y. Nosaka, S. Komori, K. Yawata, T. Hirakawa, and A. Y. Nosaka, "Photocatalytic

OH radical formation in TiO 2 aqueous suspension studied by several detection methods," *Phys. Chem. Chem. Phys.*, vol. 5, no. 20, pp. 4731–4735, 2003.

[8] A. J. Stemmler and C. J. Burrows, "Guanine versus deoxyribose damage in DNA oxidation mediated by vanadium (IV) and vanadium (V) complexes," *JBIC J. Biol. Inorg. Chem.*, vol. 6, no. 1, pp. 100–106, 2001.

[9] M. S. Elovitz and U. von Gunten, "Hydroxyl radical/ozone ratios during ozonation processes. I. The Rct concept," 1999.

[10] R. E. Huie, C. L. Clifton, and P. Neta, "Electron transfer reaction rates and equilibria of the carbonate and sulfate radical anions," *Int. J. Radiat. Appl. Instrum. Part C Radiat. Phys. Chem.*, vol. 38, no. 5, pp. 477–481, 1991.

[11] L. Wojnárovits and E. Takács, "Rate constants of dichloride radical anion reactions with molecules of environmental interest in aqueous solution: A review," *Environ. Sci. Pollut. Res.*, vol. 28, no. 31, pp. 41552–41575, 2021.

[12] O. Augusto, M. G. Bonini, A. M. Amanso, E. Linares, C. C. Santos, and S. L. De Menezes, "Nitrogen dioxide and carbonate radical anion: two emerging radicals in biology," *Free Radic. Biol. Med.*, vol. 32, no. 9, pp. 841–859, 2002.